Science of the Total Environment 1010 (2026) 181142

Contents lists available at ScienceDirect

Science of the Total Environment

journal homepage: www.elsevier.com/locate/scitotenv

Percutaneous metal absorption from airborne particulate matter: evaluating the role of skin barrier integrity

Giovanna Marussi [a,b,*], Francesca Larese Filon [a], Marta Baldassar [b], Chiara Romanello [b], Davide Porrelli [c], Marcella Mauro [a], Nicola Zingaretti [d], Gianpiero Adami [b], Matteo Crosera [b]

[a] Unit of Occupational Medicine, Department of Medicine, Surgery and Health Sciences, University of Trieste, Trieste, Italy
[b] Department of Chemical and Pharmaceutical Sciences, University of Trieste, Trieste, Italy
[c] Department of Life Sciences, University of Trieste, Trieste, Italy
[d] Clinic of Plastic and Reconstructive Surgery, Academic Hospital of Udine, Department of Medicine (DMED), University of Udine, Udine, Italy

HIGHLIGHTS

- ICP-MS and SEM-EDX used for NIST SRM 1649b metal and particle characterization.
- In vitro Franz diffusion cells assessed dermal absorption of urban dust metals.
- Damaged skin enhances transdermal metal permeation versus intact skin.
- Ni and Mn showed the highest skin penetration in both intact and damaged skin.
- As and Mo exhibited low solubility and minimal percutaneous absorption.

GRAPHICAL ABSTRACT

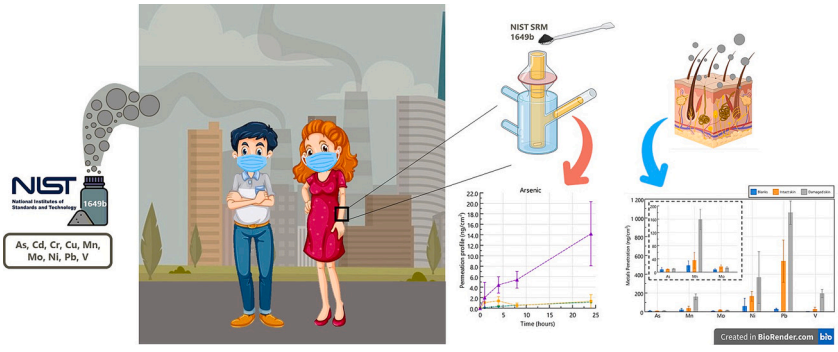

ARTICLE INFO

Keywords:
Urban dust
Heavy metals
Franz diffusion cell
Dermal exposure
Human skin

ABSTRACT

Human exposure to airborne particulate matter (PM), particularly its metal content, represents a growing public health concern due to its potential toxicological effects. While inhalation is generally considered the main exposure route, dermal absorption remains insufficiently explored. This study examined the in vitro percutaneous penetration of selected metals (As, Cd, Cr, Cu, Mn, Mo, Ni, Pb, V) from certified urban road dust (NIST SRM® 1649b) using human skin under both intact and abraded conditions. The particles were applied as a 1 % *w/v* suspension in artificial sweat medium (pH 4.5), and Franz diffusion cells were used to evaluate metal permeation over 24 h. Complementary solubility tests in simulated sweat solution buffered topH 4.5 and 6.5 showed negligible pH dependence. Scanning electron microscopy revealed submicron primary particles (mean diameter 1.19 ± 0.78 μm) with a high tendency to form agglomerates, accounting for discrepancies with the hydrodynamic size reported in the SRM certificate. No detectable skin absorption was observed for Cd, Cr, and Cu, while the remaining metals showed enhanced permeation in damaged skin, confirming the role of barrier disruption in facilitating transdermal transport. Ni, Pb, and Mn exhibited the highest permeation levels, raising concern due to their sensitizing and toxic potential. These findings provide novel insights into the dermal bioavailability of PM-associated metals and highlight the importance of including skin exposure as a relevant

* Corresponding author at: Unit of Occupational Medicine, Department of Medicine, Surgery and Health Sciences, University of Trieste, Trieste, Italy.
E-mail address: giovanna.marussi@units.it (G. Marussi).

https://doi.org/10.1016/j.scitotenv.2025.181142
Received 26 June 2025; Received in revised form 20 November 2025; Accepted 2 December 2025
Available online 8 December 2025

pathway in environmental health risk assessments, especially for populations with compromised skin integrity or in high-exposure occupational settings.

1. Introduction

The severe consequences associated with elevated air-pollution exposure became evident in the mid-20th century with events such as the 1952 London Fog, which caused numerous deaths and hospital admissions. Nowadays, air pollution - including Particulate Matter 2.5 (PM2.5), ozone (O_3), and indoor air pollution - remains a major and growing public health concern. Scientific evidence, primarily from North America and Western Europe, has linked urban airborne contamination to a wide array of health issues, from eye irritation to premature mortality (Cohen et al., 2004; Health Effects Institute, 2024).

Particulate matter (PM) consists of a heterogeneous and evolving assemblage of particles differing in size, chemical composition, and source (Kaonga et al., 2021). Among its constituents, metals and metalloids such as lead (Pb), arsenic (As), cadmium (Cd), chromium (Cr), nickel (Ni), and manganese (Mn) are of particular concern due to their capacity to induce both localised skin effects and systemic toxicity upon chronic exposure (Kelly and Fussell, 2012; Dai et al., 2015; Roy et al., 2022).

Particle size further modulates exposure pathways: PM2.5 and ultrafine particles not only penetrate deeply into the respiratory tract but can also interact with the skin barrier and, under certain conditions, cross it (Song et al., 2011; Kim et al., 2021). Although inhalation is the dominant exposure route for PM (Jin et al., 2018), dermal absorption is increasingly recognised as a non-negligible pathway for some toxicants, particularly when skin integrity is compromised or when bioaccessible ionic species are generated at the skin surface (Larese Filon et al., 2016; Dijkhoff et al., 2020). Another critical factor influencing percutaneous metal absorption is metal speciation and oxidation state (Avasarala, 2021; Larese et al., 2007). The chemical form in which a metal occurs determines its solubility, reactivity, and interaction with the skin barrier, thereby influencing its sensitizing potential and the proportion of bioaccessible and soluble ions capable of penetrating the epidermis. For instance, arsenic uptake and retention are highly influenced by its chemical form, particularly with arsenite (As(III)) being more mobile and permeable than pentavalent arsenate (As(V)) (Ouypornkochagorn and Feldmann, 2010). The speciation of chromium is highly dependent on pH. Marin Villegas and Zagury (Marin Villegas and Zagury, 2023b) showed that at pH 6.5, chromium occurs in roughly equal proportions of Cr(III) and Cr(VI), whereas at pH 4.7 the trivalent form predominates. Lead speciation also critically determines its dermal bioavailability: soluble Pb^{2+} species penetrate the skin more efficiently than insoluble oxides or metallic forms (Sun et al., 2002; Pan et al., 2010).

The skin – comprising the epidermis, dermis, and cutaneous structures (sweat glands, sebaceous glands, and hair follicles) – represents both a barrier and a potential portal for systemic uptake, especially in the presence of sweat or cleansing agents that alter metal speciation and solubility (World Health Organization, 2006; Chaparro et al., 2018; Guy, 1999; Larese Filon, 2018). Experimental work has demonstrated follicular penetration of PM and PM-induced cutaneous inflammation in animal models, and epidemiological studies have linked PM exposure to exacerbation of atopic dermatitis and accelerated extrinsic skin ageing (Jin et al., 2018; Dijkhoff et al., 2020; Vierkötter et al., 2010).

Studying dermal exposure to urban dust is particularly important, as modern cities are becoming increasingly densely populated, and industrial and commercial activities continue to expand, leading to higher pollution levels. Despite recent progress, key knowledge gaps remain. Many studies focus on single metals or simplified matrices, such as salts and nanoparticles (Crosera et al., 2016; Filon et al., 2009), with comparatively few employing real environmental samples (Larese Filon et al., 2025; Rizzo et al., 2024, 2025; Marin Villegas and Zagury, 2023a). Moreover, quantitative links between in vitro bioaccessibility and likely in vivo systemic uptake remain underdeveloped, limiting risk-based extrapolation.

This study contributes to closing this environmental health gap by examining the dermal uptake of multiple metals (As, Cd, Cr, Cu, Mn, Mo, Ni, Pb, V) from NIST SRM® 1649b urban dust using in vitro human skin models.

The objectives are to quantify the dissolution of metals from urban dust in artificial sweat at different pH levels and evaluate their percutaneous absorption through intact and damaged human skin. By integrating dissolution and permeability data, this study provides realistic and standardised information to improve understanding of exposure pathways relevant to urban air pollution and human health. Furthermore, the quantitative data generated offer a valuable basis for developing future risk assessment and exposure models.

2. Material and methods

2.1. Chemicals

All reagents employed were of analytical grade. Urea, sodium chloride (NaCl), disodium hydrogen phosphate (Na_2HPO_4), and potassium dihydrogen phosphate (KH_2PO_4) were obtained from Carlo Erba (Milan, Italy); ammonium hydroxide (NH_4OH) (25 % *w/v*) was sourced from J.T. Baker (Deventer, Netherlands); lactic acid (90 % *v*/v) was supplied by Acros Organics (Geel, Belgium); hydrogen peroxide (H_2O_2) 30 % Suprapur® and nitric acid (HNO_3) (67–69 % v/v) were procured from Merck VWR (Milan, Italy). Ultrapure water was produced using a Milli-Q system (Millipore, USA).

The physiological solution used as the receptor fluid was prepared by dissolving 2.38 g of Na_2HPO_4, 0.19 g of KH_2PO_4, and 9 g of NaCl in 1 L of MilliQ water, adjusting the pH to 7.35.

The solvent for the donor solution was synthetic sweat, prepared following the European reference method EN 1811 (European Committee for Standardization (CEN), 2011): 0.1 % w/v lactic acid, 0.1 % urea, and 0.5 % NaCl, in 100 mL of MilliQ water. This solution was divided into two 50 mL aliquots, and the pH of each portion was adjusted separately to 4.5 and 6.5 using 1 N NH_4OH.

2.2. Characterization of NIST SRM® 1649b

Standard Reference Materials (SRMs) provided by the National Institute of Standards and Technology (NIST) are widely used to simulate airborne PM exposure in vitro and in vivo.

In the present work, NIST SRM® 1649b was used. The specimen was collected in Washington, DC during 1976 and 1977 via a custom-designed baghouse. The material originates from the same bulk source as SRM® 1649 and SRM® 1649a, but sieved to obtain smaller particle sizes, leading to variations in the concentrations of target analytes. Particle size distribution measurements, conducted with laser diffraction (LD) (Mastersizer 3000, Malvern Instruments, Southborough, MA) and liquid suspension method, showed a mean particle diameter around 24.3 μm, reported as an indicative, non-certified value.

2.2.1. Microwave digestion

Prior to the in vitro test, metal concentrations in the powder were quantified and compared with the values in the certificate of analysis of the standard. Three aliquots of urban powder (average 0.0511 ± 0.0003 g) were treated with 3 mL of HNO_3 and 1 mL of H_2O and digested in a microwave oven (Multiwave-PRO, Anton Paar) at 180 °C for 20 min, following modified EPA Method 3052 (US EPA, 1996). After cooling, the

vessel contents were diluted to 20 mL using Milli-Q water and filtered (0.45 μm pore size, Millipore Millex HA). Samples were diluted 1:50 with MilliQ water before analysis.

2.2.2. SEM-EDS characterization

The morphology and particle size distribution of NIST SRM® 1649b were analysed by Scanning Electron Microscopy coupled with Energy Dispersive Spectroscopy (SEM-EDS). For the analysis, the powder was mounted on aluminium stubs using carbon double-sided adhesive tape and coated with a thin carbon layer via pulsed carbon rod evaporation (Quorum Q150T ES Plus sputter coater, Quorum Technologies Ltd., Lewes, UK). Imaging was performed with a Gemini300 SEM (Zeiss, Oberkochen, Germany) coupled with a Bruker XFlash 610 M EDS probe, operating with secondary and backscattered electrons at a working distance of 8.6 mm and an acceleration voltage of 5 kV.

2.3. Dissolution test in synthetic sweat solutions

The bioavailability and dermal uptake of metals largely depend on their solubility and speciation under physiological conditions. According to OECD (2018) guidance, in vitro dissolution tests in simulated biological fluids are essential to estimate the soluble, bioaccessible fraction before assessing percutaneous absorption. Therefore, metal dissolution in two artificial sweats (pH 4.5 and pH 6.5) was evaluated prior to the skin permeation experiments, adapting the protocol reported by Magnano et al. (2022).

Three replicates were prepared by dispersing 0.1 g of NIST SRM® 1649b in 10 mL of artificial sweat (1 % *w/v*) at the two different pH values. Metal dissolution was monitored periodically by collecting 1.0 mL aliquots after 1, 8 and 24 h. The obtained samples were frozen until analysis with ICP-MS. At the time of analysis, thawed samples were diluted 1:20 with MilliQ water and filtered (0.22 μm pore size, Millipore Millex HA).

2.4. Human skin handling and preparation

Full-thickness human abdominal skin was sourced from surgically removed tissue (donors aged 45–65 years, both sexes). The subcutaneous fat layer was carefully excised with a scalpel, and any hair on the epidermis was shaved. Abdominal skin samples were stored at −25 °C for a period not exceeding four months.

On the day of the experiment, skin samples were thawed at room temperature in physiological solution and cut into 2 × 2 cm square sections. Skin thickness, measured using a Vernier calliper, did not exceed 1 mm.

Skin integrity was assessed following the procedure described by Magnano et al. (2022), using Transepidermal Water Loss (TEWL) as the evaluation parameter.

In vitro tests were conducted as follows:

Exp.1 - Blanks controls: Skin samples to which no urban dust powder was applied; only the artificial sweat medium at pH 4.5 was used as the donor phase.

Exp.2 - Intact skin: Untreated skin samples exposed to the donor phase consisting of 1 % *w/v* urban dust powder in synthetic sweat solution at pH 4.5.

Exp. 3 - Damaged skin: skin samples prepared using an abrasion protocol based on the method described by Bronaugh and Stewart (1985), in which a 19-gauge hypodermic needle was used to create six parallel and six perpendicular scratches on the skin surface; these were similarly exposed to the 1 % w/v urban dust donor solution.

Three diffusion cells were used as blank controls, four cells for intact skin, and four for damaged skin. The experiment was repeated twice, resulting in a total of 22 independent cells.

2.5. Preparation of the in vitro diffusion system

Skin absorption experiments were conducted using static diffusion cells in compliance with OECD guidelines (OECD, 2004). The study applies a conceptual model linking metal speciation and dissolution kinetics to transdermal flux governed by Fickian diffusion and is influenced by the integrity of the skin barrier. Parallel exposures were carried out in Franz-type static diffusion cells featuring an 11 mm diameter orifice, corresponding to an exposed surface area of 0.95 cm^2. Each piece of skin was positioned between the donor and receptor compartments, with the stratum corneum (SC) oriented towards the donor chamber.

The receptor chamber - with an average volume of 4.5 mL - was filled with a physiological solution was kept under continuous agitation with a Teflon-coated magnetic stir bar. Temperature was maintained at 32 ± 1 °C through a thermostated water circulation system surrounding the cells.

The donor chamber held 1.0 mL of a freshly prepared 1 % *w/v* urban dust suspension in artificial sweat medium (pH 4.5), applied directly contact onto the skin surface. To ensure a homogeneous dispersion of the powder, the suspension was subjected to ultrasonic treatment for 10 min before application. The corresponding applied dose was $Q_0 = 10.5$ mg/cm^2.

2.6. Permeation test

The permeation study was conducted over a 24-hour period to quantify the amount of each metal retained within the skin.

At selected time points (1, 4, 8, and 24 h), 0.5 mL of the receiving solution was removed with insulin syringes. The receptor compartment was replenished with 0.5 mL of fresh physiological solution after every sample collection to maintain a constant volume and ensure optimal contact of the solution with the dermis. The collected samples were acidified with nitric acid and frozen until analysis. For ICP-MS analysis, the samples were diluted 1:10 with MilliQ water.

At the conclusion of the 24-hour exposure period, the diffusion cells were disassembled. Donor and receptor solutions were collected and frozen for further analysis. Any unabsorbed powder remaining on the skin surface was removed by washing the donor chamber three times with 1.0 mL of MilliQ water. Additional rinses were performed to ensure complete removal of dust residues from the skin that could lead to an incorrect quantification, the surface was cleaned with a cotton bud.

The skin was then removed from the in vitro diffusion system, trimmed to preserve only the part exposed to the donor solution, wrapped in Parafilm and stored in the freezer at −25 °C until digestion treatment (see Section 2.7).

2.7. Microwave digestion of skin samples

To determine the concentration of metals potentially retained in the skin, tissue mineralisation was performed to destroy the organic material in the sample. Epidermis and dermis were separated by immersion in Milli-Q water at 60 °C for 2 min (for damaged skin, separation was not feasible).

The resulting samples were weighed and placed in Teflon digestion vessels with 3 mL of HNO_3, 0.50 mL of H_2O_2 and 1.0 mL of MilliQ water, following modified EPA Method 3052 (US EPA, 1996). Microwave digestion of the mixture was carried out at 180 °C for 20 min using a Multiwave-PRO system (Anton Paar). After this step, MilliQ water was added to reach a final volume of 20 mL. For ICP-MS analysis, samples were further diluted 1:10 with MilliQ water.

2.8. ICP-MS analysis

Metal concentrations (As, Cd, Cr, Cu, Mn, Mo, Ni, Pb, V) in the obtained samples was performed using Inductively Coupled Plasma - Mass Spectrometry (ICP-MS) with a NexION 350× Spectrometer

(PerkinElmer, USA), featuring an ESI SC Autosampler. Measurements were carried out in Kinetic Energy Discrimination (KED) mode with ultra-high purity helium at a flow rate of 4.8 mL/min to reduce polyatomic ion interferences generated in the collision cell. Scandium (Sc), Yttrium (Y), and Holmium (Ho) were included as internal quality control standards to assess potential matrix effects and to minimise volume inaccuracies.

Calibration was achieved using a 6-point series (0.5, 1, 5, 10, 100 and 500 μg/L) prepared by adequate dilution of "Periodic table mix 1" and "Periodic table mix 2" (TraceCERT®, Merck, Germany). Sample quantification was based on the linear calibration curve (range: 0.5–500 μg/L; $R^2 = 0.99$). Limits of Quantification (LOQ) for each element were as follows: As (75 u.m.a.) 0.03 μg/L; Cd (111 u.m.a.) 0.02 μg/L; Cr (52 u.m.a.) 0.01 μg/L; Cu (63 u.m.a.) 0.01 μg/L; Mn (55 u.m.a.) 0.01 μg/L; Mo (98 u.m.a.) 0.01 μg/L; Ni (60 u.m.a.) 0.02 μg/L; Pb (208 u.m.a.) 0.01 μg/L; and V (51 u.m.a.) 0.01 μg/L. Repeatability, reported as relative standard deviation (RSD%), was <3 %.

2.9. Statistical analysis

Data processing was conducted using Microsoft Excel (2019) and Stata (version 11.0; StataCorp LP, College Station, TX, USA). Graphs and plots were generated using LabPlot (version 2.12.1). Cumulative metal concentrations permeated at each time point are expressed as mass per unit area of skin (ng/cm^2). The amount of metals retained in the skin after 24 h was also calculated. All data were presented as mean ± standard deviation (SD). Differences among independent datasets were assessed using the Mann-Whitney *U* test, with *p*-values ≤0.05 considered as statistically significant.

3. Results

3.1. Characterization of NIST SRM® 1649b

The elemental composition of NIST SRM® 1649b was determined by ICP-MS to quantify the target elements, including arsenic and molybdenum, which are not listed in the CRM certificate of analysis. The average concentrations of As, Cd, Cr, Cu, Mn, Mo, Ni, Pb, and V in NIST SRM® 1649b are presented in Table 1.

The measured values were compared with the reference values reported in the certificate of analysis. Satisfactory recoveries were achieved, ranging from 88 to 119 %, indicating negligible matrix effects, except for Cr, which showed a recovery of 77 %. This lower value is probably due to the absence of hydrofluoric acid during microwave digestion, resulting in incomplete solubilisation of Cr bound to silicate matrices and partial analyte loss.

Representative SEM-EDX images of urban dust powder (NIST SRM® 1649b) and its size distribution, are presented in Fig. 1.

Scanning Electron Microscopy (SEM) revealed that the particles in the powder had an average diameter of 1.19 ± 0.78 μm (number of particles measured = 300), exhibited heterogeneous morphologies, and tended to form larger aggregates.

The NIST SRM® 1649b certificate of analysis reported that the measurement was conducted in ethanol with Triton X-100 surfactant at 0.01 % concentration, by using a laser diffraction instrument (Mastersizer 3000, Malvern Instruments, Southborough, MA). The discrepancy between the particle size measured in this study and the average diameter reported in the SRM certificate (24.3 μm) is likely attributable to methodological differences. In fact, laser diffraction estimates particle size based on the angular variation in light scattering, assuming spherical particles and reporting a volume-equivalent diameter. This method analyses a large number of particles, providing a volume-weighted distribution that can overrepresent larger particles. In contrast, SEM provides direct imaging of particles, allowing for geometric measurements on a number basis, often limited to smaller sample sets. Differences in sample preparation, such as dispersion in liquid for laser diffraction versus dry deposition for SEM, and the presence of agglomerates or irregular shapes, may also contribute to discrepancies between the two methods.

Table 1
Comparison of reference values (mg/kg ± SD) provided in the NIST SRM® 1649b certificate of analysis and the concentrations obtained via ICP-MS analysis of the same material. Elements considered: Pb, V, Cr, Mn, Ni, Cu, As, Mo, and Cd.

	Certified mass fraction (mg/kg)	Obtained mass fraction (mg/kg)	% recovery
Pb	12,864 ± 62	14,211 ± 590	110
V	344 ± 9	372 ± 14	108
Cr	210 ± 4	161 ± 7	77
Mn	337 ± 4	297 ± 13	88
Ni	168 ± 6	178 ± 7	106
Cu	311 ± 7	288 ± 12	93
As	–	87.2 ± 4.7	–
Mo	–	16.2 ± 0.9	–
Cd	26.10 ± 0.28	31.14 ± 1.50	119

3.2. Dissolution tests

Since the solvent could significantly influence metal diffusivity and bioavailability (Hostynek, 2003), preliminary dissolution tests must be performed. These aim to determine the percentage of metals that solubilise in sweat at two different pH levels (4.5 and 6.5). In fact, the presence of sweat on the skin promotes the release of metal ions, which can pass through the stratum corneum and penetrate the dermis reaching the systemic circulation (Franken et al., 2015; Larese Filon, 2018). While human sweat typically has a pH between 5.0 and 5.5, it may decrease to values below 4.0 during physical exertion, thereby enhancing metal oxidation and cutaneous absorption. For this reason, a synthetic sweat solution at pH 4.5 was used as the donor phase in the permeation test.

The dissolution rates of the investigated metal ions (Table 2) were calculated from the concentrations reported in the certificate of analysis of NIST SRM® 1649b (Table 1, Section 3.1).

Chronic exposure to even low metal concentrations can trigger allergic responses, particularly for skin sensitizers such as Ni and Cr, making all the detected concentrations significant (Thyssen and Menné, 2010).

Both skin sensitizers, Cr and Ni, followed the same trend: after 1 h, a dissolution rate of 42.5 μg/L for Cr and 510 μg/L for Ni was reached at pH 4.5, and these values remained fairly constant thereafter. An overall increase in the concentration of these two metals was noted in the synthetic sweat at pH 4.5, while for the solutions at pH 6.5, the maximum was reached after 8 h. By comparing the obtained concentrations of the skin sensitizers in the two synthetic biological fluids, the results were comparable, thus inferring that there is no particular pH dependency. This finding aligns with previous study in which the dissolution of metal species from road dust was investigated, obtaining a low dependence of dissolution on pH (Magnano et al., 2022). Although Cr and Ni were present in similar concentrations in the NIST SRM® 1649b, nickel concentrations in solution were approximately tenfold higher than chromium, suggesting a greater solubility of Ni under these particular conditions.

Among the toxic metals (As, Cd, Pb), arsenic demonstrated a gradual increase in solubility over time, with comparable results in both synthetic sweat solutions. In contrast, cadmium and lead reached steady concentrations within 1 h of exposure (183.8 μg/L and 19.43 mg/L at pH 4.5, respectively), showing no significant variation up to 24 h. Cd and As showed slightly higher values in the case of synthetic sweat at pH 6.5, whereas Pb had the opposite behaviour with a dissolution rate of 13.5 % at pH 4.5 versus 10.6 % at pH 6.5: this is consistent with the known inverse correlation between Pb solubility and pH (Chaparro

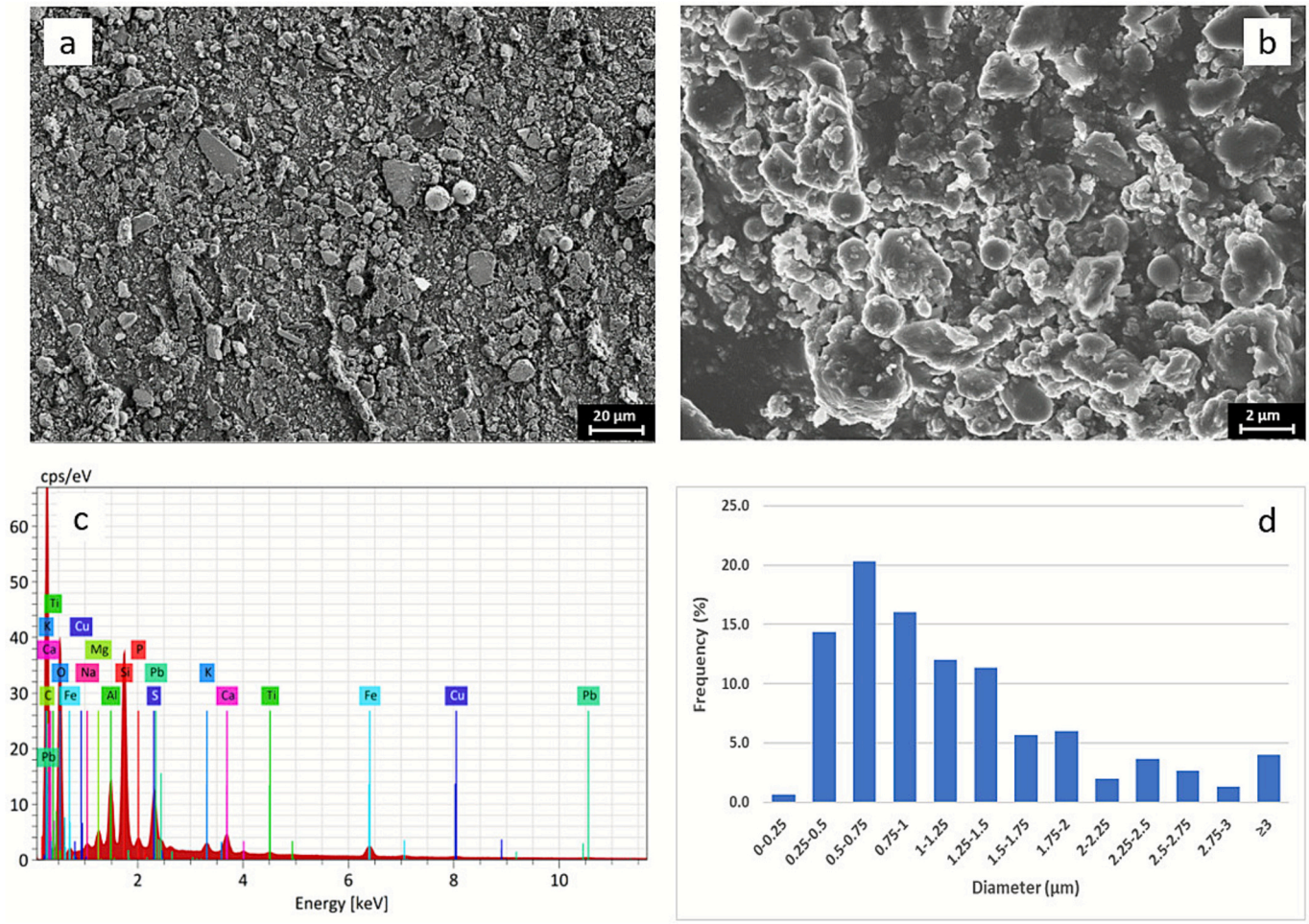

Fig. 1. SEM-EDX images of NIST SRM® 1649b at a magnification of 1000× (a) and 10,000× on (b). EDX average spectrum (c) and histograms showing the distribution of number of particles according to their size (d).

Table 2
Bioavailability of As, Cd, Cr, Cu, Mn, Mo, Ni, Pb, and V from NIST SRM® 1649b in synthetic sweat formulations at pH 4.5 and 6.5. Data are expressed as percentage (% ± SD), obtained by relating dissolution rates (µg/g) to mass fraction in mg/kg reported in the NIST certificate of analysis.

	Synthetic sweat solution at pH 4.5			Synthetic sweat solution at pH 6.5		
	1 h	8 h	24 h	1 h	8 h	24 h
% As	8.63 ± 1.14	10.06 ± 1.98	11.32 ± 0.74	9.04 ± 0.59	11.37 ± 0.36	11.22 ± 0.28
% Cd	69.37 ± 10.38	74.32 ± 15.52	73.87 ± 3.71	72.39 ± 2.36	83.83 ± 1.97	74.48 ± 1.40
% Cr	1.99 ± 0.35	2.21 ± 0.48	2.35 ± 0.18	1.89 ± 0.07	2.39 ± 0.07	2.28 ± 0.02
% Cu	13.62 ± 1.88	15.08 ± 2.95	16.01 ± 1.34	13.31 ± 0.98	15.74 ± 0.48	14.73 ± 0.46
% Mn	32.05 ± 5.06	33.81 ± 7.08	34.29 ± 2.81	33.55 ± 1.77	38.43 ± 1.13	34.13 ± 0.70
% Mo	14.87 ± 2.16	21.92 ± 4.72	26.24 ± 2.23	15.82 ± 0.97	26.21 ± 0.45	27.36 ± 1.03
% Ni	29.92 ± 4.62	31.19 ± 6.32	31.71 ± 2.56	30.78 ± 1.86	34.91 ± 1.11	31.23 ± 0.55
% Pb	14.88 ± 2.97	16.04 ± 5.36	13.60 ± 1.29	11.71 ± 1.18	13.52 ± 0.25	9.50 ± 0.28
% V	30.14 ± 4.88	33.96 ± 7.41	36.03 ± 3.05	29.23 ± 1.33	35.41 ± 1.47	32.66 ± 0.81

et al., 2018).

Molybdenum behaved similarly to arsenic, showing increasing solubility up to 8 h and subsequent stabilisation, with negligible pH effects.

Manganese, copper, and vanadium followed a similar profile to the skin sensitizers, maintaining relatively constant concentrations throughout the 24-hour dissolution period and showing no appreciable differences between the two pH values.

Therefore, a common solubility profile was observed across both synthetic sweat solutions. Although the overall dissolution behaviour was similar at both pH levels (4.5 and 6.5), the use of synthetic sweat at pH 4.5 as the donor phase in the in vitro absorption test enables direct comparison with earlier studies (Magnano et al., 2022; Larese Filon et al., 2025).

In conclusion, as all metals tested during the dissolution experiment were present in quantifiable amounts, it was decided to consider all elements in the subsequent skin permeation tests, including essential trace elements such as Mn and Mo (Carvalho and Coelho, 2015).

Based on 24-hour metal concentrations (µg/L) measured in the dissolution tests, the effective dose (µg/cm^2) was calculated by considering the donor phase volume and the exposed skin surface. Table 3 presents the actual doses of each metal, alongside the theoretical doses derived from the NIST SRM® 1649b certificate of analysis.

3.3. *In vitro skin absorption studies*

Metal permeation through the skin is influenced by several factors, including donor-phase concentration, metal solubility, intrinsic diffusivity across the stratum corneum, and affinity for skin tissues. Notably, a high affinity for skin components may result in reduced translocation to the receptor phase due to metal retention within the skin layers

Table 3
Theoretical and effective doses of the metals under study. Effective doses were calculated based on a donor solution volume of 1.0 mL of donor solution and an exposed skin surface area of 0.95 cm^2.

	Theoretical dose (μg/cm^2)	Effective dose (μg/cm^2)
As	0.92 ± 0.05	0.11 ± 0.01
Cd	0.27 ± 0.01	0.21 ± 0.01
Cr	2.21 ± 0.04	0.05 ± 0.01
Cu	3.27 ± 0.07	0.53 ± 0.04
Mn	3.55 ± 0.04	1.23 ± 0.09
Mo	0.17 ± 0.01	0.05 ± 0.01
Ni	1.77 ± 0.06	0.57 ± 0.04
Pb	135 ± 0.7	18.7 ± 1.6
V	3.62 ± 0.09	1.32 ± 0.10

(Larese Filon, 2018).

In this study, transdermal absorption of As, Cd, Cr, Cu, Pb, Mn, Mo, Ni, and V from urban particulate matter was evaluated. A suspension of urban dust (1 % *w/v* of NIST SRM® 1649b) was freshly prepared, and 1.0 mL was applied to the skin surface, resulting in metal deposition rates reported in Table 3 (Section 3.2). The experiment was conducted using excised human skin mounted on Franz diffusion cells over a 24-hour exposure period. This methodology, recommended by the Organization for Economic Co-operation and Development (OECD, 2004), is widely accepted as a reliable in vitro model for predicting in vivo permeation of topical products (Franz et al., 2009).

To simulate compromised barrier conditions, abraded skin was employed to mimic conditions such as dermatitis, superficial wounds, or sunburn. Metals penetration was evaluated in both intact and damaged skin to assess differential behaviour under altered barrier integrity.

Following 24 h of exposure, the concentrations of the target metals were quantified in both the receptor fluid and skin layers. Cadmium remained below the instrumental limit of detection (LOD), while chromium and copper showed no statistically significant differences among blank, intact, and damaged skin samples. Consequently, Cd, Cr, and Cu were excluded from further data interpretation.

3.3.1. Permeation in the receptor fluid

By analysing the samples from the receptor compartment, it was possible to assess the amount of metal ions that permeated through the skin barrier and could, in theory, reach the bloodstream and undergo systemic distribution. Concentrations of As, Mn, Mo, Ni, Pb, and V in the receptor compartment, expressed in ng/cm^2, are showed in Table 4 (24 h values) and Fig. 2 (permeation profiles).

Nickel was detected as early as 1 h after exposure, with relatively constant concentrations over time. As shown in Table 4, Ni levels were comparable in both intact and damaged skin (approximately 30 ng/cm^2), indicating its ability to permeate the skin independently of barrier integrity. This behaviour suggests that Ni may follow a different permeation mechanism or interact more favourably with the skin matrix compared to other metals. These results differ from those observed in the previous study on road dust (Magnano et al., 2022), where nickel permeation was more pronounced in injured skin.

Table 4
Concentrations of As, Mn, Mo, Ni, Pb, and V (ng/cm^2) in the receptor medium for blanks, intact, and damaged skin. Asterisks (*) indicate statistically significant difference ($p < 0.02$) between blanks and either intact or damaged skin (Mann-Whitney test); daggers (†) indicate significant differences ($p < 0.02$) between intact and damaged skin.

	As (ng/cm^2)	Mn (ng/cm^2)	Mo (ng/cm^2)	Ni (ng/cm^2)	Pb (ng/cm^2)	V (ng/cm^2)
Blank	1.16 ± 0.6*	4.36 ± 3.38*	1.00 ± 0.4*	8.41 ± 4.36*	0.58 ± 0.18*	4.70 ± 2.96*
Intact skin	1.32 ± 1.26†	8.87 ± 1.84†	1.06 ± 0.15†	29.2 ± 19.4	3.36 ± 0.73†	6.37 ± 1.28†
Damaged skin	14.2 ± 6.1*†	66.8 ± 29.2*†	5.57 ± 2.30*†	27.3 ± 12.6*	8.53 ± 4.81*†	21.3 ± 10.3*†

In contrast, arsenic and lead displayed a clear dependence on skin integrity. After 24 h of exposure, As concentrations were 1.3 ng/cm^2 for intact skin and 14 ng/cm^2 for damaged skin, while Pb concentrations reached 3.4 ng/cm^2 and 8.5 ng/cm^2, respectively. These findings confirm the protective role of the skin barrier. Lead results were consistent with those previously reported for road dust, where similar permeation levels (approximately 6 ng/cm^2) were observed in damaged skin. Furthermore, as displayed in Fig. 2, arsenic showed no significant differences between the concentrations of blanks and intact skin, suggesting that the skin effectively inhibits its permeation under non-compromised conditions.

The barrier function of the skin was also observed for molybdenum and vanadium, which followed the same trend as arsenic, with permeation profiles in the intact skin overlapping those of blanks (blanks and intact skin respectively for Mo: 1.0 ng/cm^2 vs 1.1 ng/cm^2; V: 4.7 ng/cm^2 vs 6.4 ng/cm^2 at 24 h). Conversely, manganese exhibited a distinct pattern: in intact skin, Mn levels in the receptor fluid were approximately twice those of the blanks and about seven times lower than those of damaged skin. For damaged skin, the concentrations in the receptor compartment at 24 h were approximately 70 ng/cm^2 for Mn (the highest value), around 6 ng/cm^2 for Mo, and 21 ng/cm^2 in the case of V. These findings are in line with previously reported data on road dust permeation.

When comparing the permeation profiles of all metals, it is noteworthy that although the initial concentration of lead was the highest (effective dose: 18.7 μg/cm^2), the amount of Pb found in the receptor compartment was lower than that of other metals such as As, Mn, and Ni. This indicates a higher retention or binding affinity of Pb within the skin matrix, which limits its systemic absorption, even when the skin barrier is compromised. Ni showed the highest permeation (approximately 28 ng/cm^2) with no significant differences between intact and damaged skin, whereas all other metals displayed significantly higher permeation when the barrier was compromised.

3.3.2. Penetration in the skin

Metal penetration was examined in both intact and damaged skin to assess their behaviour under different skin conditions (see Fig. 3 and Table 5).

In intact skin, the highest total metal absorptions were observed for Pb (539 ng/cm^2) and Ni (164 ng/cm^2), while As and Mo exhibited the lowest values (8.6 ng/cm^2 and 16.2 ng/cm^2, respectively). In damaged skin, total absorption increased compared to intact skin for V, Ni, Mn and Pb, while penetration of As and Mo remained within the same order of magnitude as in intact skin. These findings suggest that for the former group of metals, compromise of the skin barrier significantly facilitates transdermal absorption, supporting prior observations (Kezic and Nielsen, 2009). In contrast, no statistically significant differences were found for As and Mo between intact and damaged skin, indicating a lesser dependency on barrier integrity. Additionally, analysis of blank samples for these two elements demonstrated comparable concentrations to those measured in both intact and damaged skin, further supporting the limited dermal penetration of As and Mo under the tested conditions. It should be noted that, due to the inherent inter-individual variability in skin absorption experiments, achieving statistical significance can be challenging, particularly when evaluating trace element permeation across heterogeneous skin models. This is the case of nickel for which a statistically significant difference between cells was not achieved due to the wide variability between cells.

4. Discussion

The present work examined in vitro metal permeation from urban dust through both intact and compromised human skin. The dermal absorption of six metals (As, Mn, Mo, Ni, Pb, and V) was evaluated using

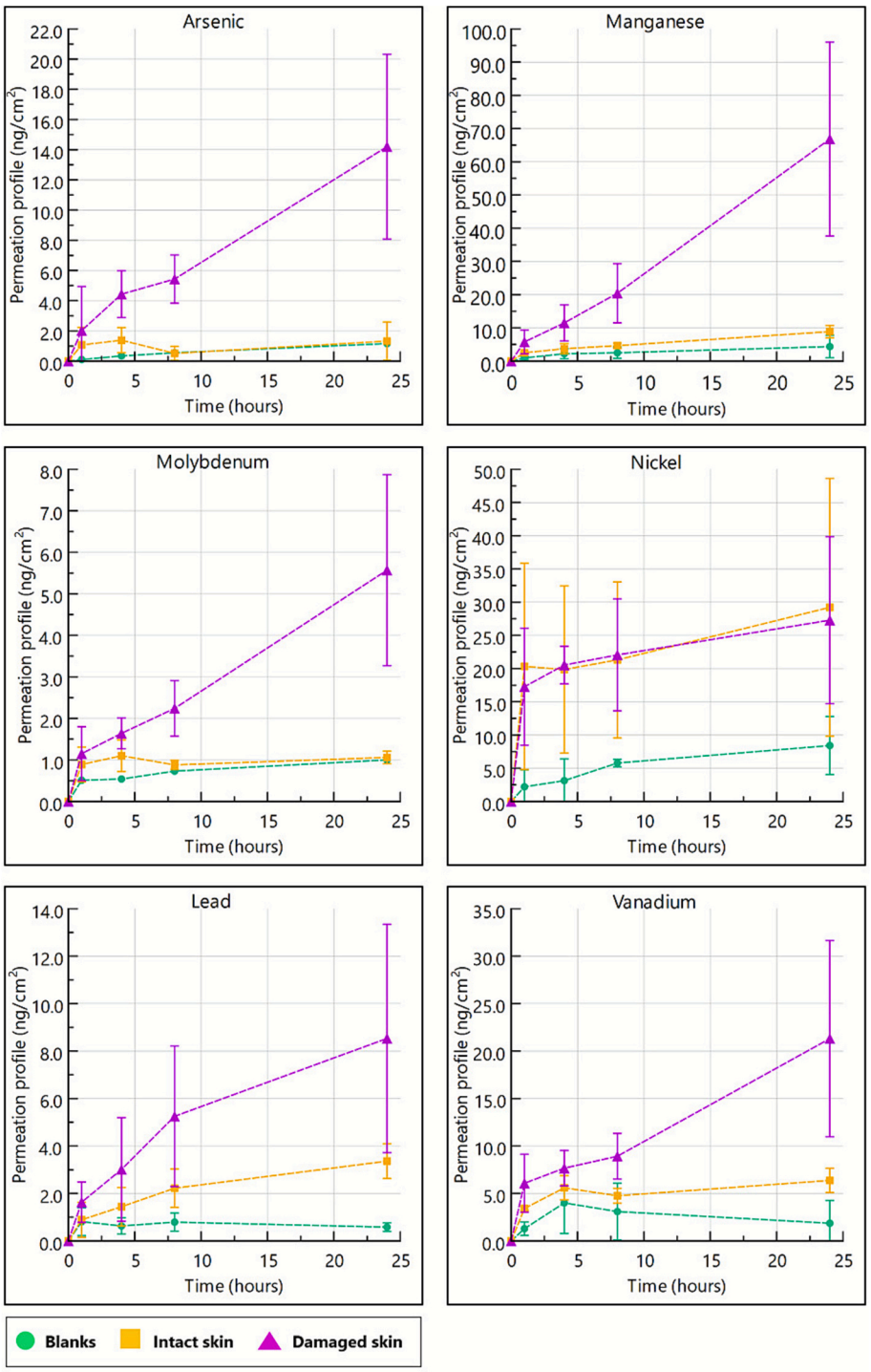

Fig. 2. Permeation profiles of As, Mn, Mo, Ni, Pb, and V (ng/cm^2) in the receptor compartment for blanks, intact and damaged skin (exposure time 24 h).

Franz static diffusion cells. It is well established that metal ions and their salts can penetrate the stratum corneum, reach the dermis, and potentially enter systemic circulation (Larese Filon, 2018; Franken et al., 2015). Upon contact with the skin, metallic objects or metal powders can release ions, a process further enhanced in the presence of sweat. Consistent with the findings of Marin Villegas et al. (2019), synthetic sweat at pH 4.5 generally exhibited the highest bioavailability percentages. This outcome reflects the critical role of pH in metal permeation, as lower pH values enhance solubility and increase the degree of metal ionization, particularly for cationic species, thereby influencing their bioavailability. Accordingly, the experiment employed artificial sweat solution at pH 4.5 to replicate the typical skin pH, which generally ranges from 4 to 5.5 (Dyer et al., 1998).

Since the metal species present in dust differ in their solubilisation behaviour, dissolution test results for metals in NIST SRM® 1649b urban dust were compared with those from Magnano et al. (2022), which assessed the skin permeation of road dust using CRM BCR®-723. The road dust was sampled from the ceiling of the Tanzenberg Tunnel (Styria, Austria), approximately 50 km north of Graz, by collecting material from ventilation ducts with brooms and a vacuum cleaner. Urban dust exhibited greater metal solubility than road dust, suggesting that the chemical speciation of metal constituents differs significantly

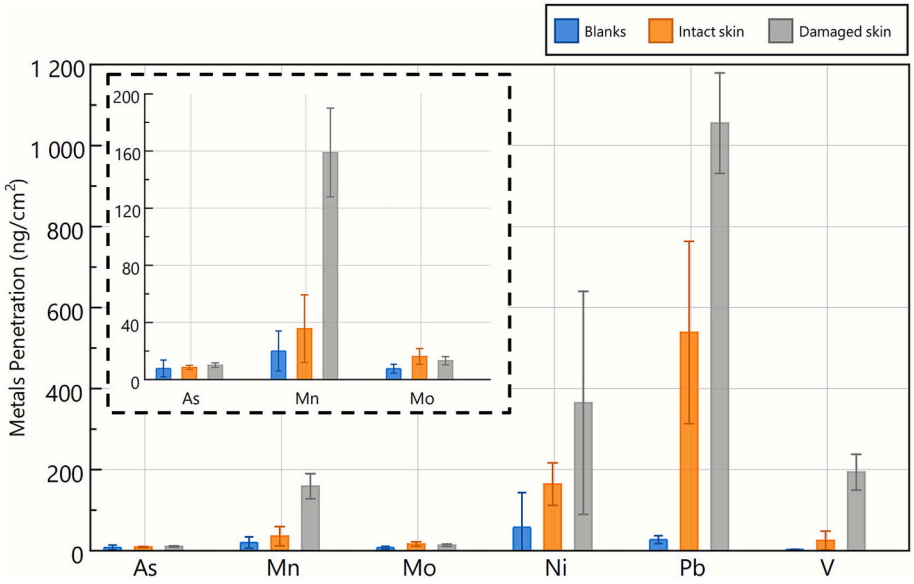

Fig. 3. Skin penetration of metals after 24 h exposure in blanks, intact and damaged human skin. The applied dose was 10.5 mg/cm^2. Data are presented as mean values, with standard deviation (SD) shown as error bars.

Table 5
Total distribution of metals in skin layers after 24 h exposure in control blanks, intact, and damaged skin. The applied dose was 10.5 mg/cm^2. Values are expressed as mean ± SD. Asterisks (*) indicate statistically significant differences between blanks and either intact or damaged skin (Mann–Whitney test, $p < 0.02$); daggers (†) indicate statistically significant differences between intact and damaged skin ($p < 0.02$).

	As (ng/cm^2)	Mn (ng/cm^2)	Mo (ng/cm^2)	Ni (ng/cm^2)	Pb (ng/cm^2)	V (ng/cm^2)
Blanks	7.8 ± 5.9	20.0 ± 14.0*	7.6 ± 3.1*	57.8 ± 85.4	27.1 ± 9.7*	2.9 ± 0.5*
Intact skin	8.6 ± 1.4	35.6 ± 23.7†	16.2 ± 5.5*	164.2 ± 52.4	538.5 ± 225.1*†	25.1 ± 23.2*†
Damaged skin	10.1 ± 1.6	159.0 ± 31.0*†	13.2 ± 2.9*	364.7 ± 275.3	1055.2 ± 123.9*†	193.7 ± 44.1*†

between matrices of similar urban origin.

Regarding the permeation test, our data indicate that – even in small quantities – metals were able to penetrate the skin relative to their donor-phase concentrations. Accumulation within the skin reflects deposition following topical application, whereas detection in the receptor fluid represents the fraction potentially available for systemic distribution. Notably, higher concentrations in the receptor fluid were found for Ni and Mn, while Mo and As exhibited minimal skin penetration.

Concerning nickel, the results closely align with the study of Larese Filon et al. (2025), who reported no statistically significant difference in receptor fluid values (59.2 ng/cm^2 for intact skin and 56.2 ng/cm^2 for damaged skin). However, Ni retention within the skin was more than twice as high in injured skin compared to intact skin, corroborating earlier works on Ni-containing powders (Filon et al., 2009; Magnano et al., 2022). Comparing the receiving phase values with the concentrations retained in the skin, an increase of almost six-fold was observed for intact skin and over thirteen-fold for damaged skin, confirming the strong affinity of the stratum corneum and upper parts of epidermis for Ni ions (Malmberg et al., 2018). Simon et al. (2024) found that Ni^{2+} and Co^{2+} penetrated the skin more efficiently than Pd^{2+} and thus may sensitize and elicit Allergic Contact Dermatitis (ACD) more easily. Nickel is a well-established sensitizer and a major cause of allergic contact dermatitis, a condition marked by erythema, vesiculation, and, in chronic cases, xerosis and desquamation (Owen et al., 2018). A recent study by Magnano et al. (2024) suggested that application of specialized barrier creams may reduce Ni permeation and accumulation within skin layers.

Manganese was the other metal detected in notable quantities in the receptor fluid for both intact and damaged conditions. Although Mn is a trace element normally present in the body at concentration of 10–29 μg (Lansdown, 1995), the values observed in this study were considerably higher than controls. In fact, Mn exhibited a dermal bioavailability of nearly 40 % after just 1 h. These findings are particularly relevant, as chronic overexposure may cause neurotoxicity through accumulation in brain regions such as the caudate nucleus and hippocampus (Erikson and Aschner, 2003; Katsnelson et al., 2015).

Regarding the toxic metals analysed (As and Pb), the levels of arsenic detected in both the receptor fluid and skin membrane were comparable to those in the blank controls. Arsenic skin penetration is influenced by charge state and mobility (Hostýnek et al., 1993; Ouypornkochagorn and Feldmann, 2010). In this study, As was likely present in the pentavalent form, which is less mobile and thus poorly absorbed. Similar conclusions were drawn by Marin Villegas and Zagury (2021), who studied the skin bioaccessibility of As, Cr, Cu, Ni, Pb, and Zn from several geological materials through in vitro experiments using two artificial sweat formulations at pH 4.7 and 6.5. At pH 4.7, they reported a 2-hour dissolution rate of As of 5.1 %, which aligns with the 1-hour dissolution value of 8.6 % observed in our study. Given this low bioavailable percentage, the minimal As amounts detected in both the receptor fluid and skin are consistent with expectations.

The other toxic element analysed in this study was lead, for which no biological function in the human body is known. It showed a progressive increase in receptor fluid concentration, reaching values of 3.36 ng/cm^2 and 8.53 ng/cm^2 in intact and damaged skin, respectively – results consistent to those reported by Julander et al. (2020). Pb levels in the skin were nearly 160-fold higher than in the receptor fluid. Moreover, a stepwise increase was observed from blank controls to intact skin samples and then damaged skin, with Pb concentrations in the latter approaching 1 μg/cm^2. These results confirm that lead can penetrate both human and animal skin under similar conditions (Stauber et al., 1994; Lilley et al., 1988; Sun et al., 2002; Filon et al., 2006; Magnano et al., 2022). Lead absorption occurs initially through sweat glands and hair follicles, followed by slower transepidermal penetration (Franken et al., 2015).

Vanadium exhibits a similar permeation profile to arsenic, with intact-skin levels comparable to controls, indicating effective barrier function. This is further supported by an almost eightfold increase in V concentration in damaged skin, alongside a threefold increase in the receptor fluid compared to intact skin. Although comparative data on V permeation are limited, this finding is notable. While trace vanadium may serve physiological roles, elevated levels are associated with hepatotoxicity and nephrotoxicity (Du et al., 2025). Moreover, some vanadium compounds are considered potentially genotoxic and have been classified as mutagenic, teratogenic, and "suspected carcinogens" (Rehder, 2013).

Regarding molybdenum, results were consistent with Larese Filon et al. (2025), who examined the skin absorption of metals after contamination with stainless steel (1 % *w/v*) resulting from the decommissioning of nuclear fusion and fission reactors. In the work of Larese Filon et al., no significant differences were noted in receptor fluid concentrations between controls and intact skin (both measuring 1.3 ng/cm^2), which closely aligns with our findings of approximately of 1 ng/cm^2. However, in the case of damaged skin, Mo concentrations increased to 2.9 ng/cm^2 in the previous study and to 5.6 ng/cm^2 in our work. Mo penetration was slightly higher in damaged (3.0 ng/cm^2) compared to intact (2.0 ng/cm^2) skin, although this difference was not statistically significant, as reported by Larese Filon et al. In our study, the concentrations detected were higher in both conditions - 16.2 ng/cm^2 in intact skin and 13.2 ng/cm^2 in damaged skin - yet no statistically significant difference was observed between the two, in line with the earlier findings.

A comparative evaluation of total metal absorption between intact and compromised skin samples revealed generally higher concentrations of metals in damaged skin. This observation reinforces the notion that disruption of the stratum corneum - due to abrasions, wounding, or dermatological conditions - significantly compromises barrier integrity and facilitates enhanced percutaneous absorption. This increased permeability heightens the risk of dermal toxicity and hypersensitivity reactions. The finding is particularly relevant for Ni, a well-known contact allergen, as even minimal exposure can elicit strong immune responses in sensitized individuals, potentially leading to allergic contact dermatitis.

In conclusion, this study provides a reproducible experimental framework integrating metal dissolution kinetics and skin permeability data to improve the estimation of dermal exposure to urban contaminants. The use of a certified reference material (NIST SRM® 1649b) ensures chemical complexity and interlaboratory comparability, offering a robust baseline for model-based exposure assessment. Although the work did not differentiate between specific oxidation states or chemical species, this standardised approach remains appropriate for complex dust matrices, where multiple metal forms coexist as they do in real environmental samples. Such in vitro data provide essential benchmarks for refining predictive exposure models. Future studies combining speciation analyses with real-world urban dust could further enhance the accuracy of dermal risk assessments by integrating local particulate composition, exposure frequency, and adherence factors.

5. Conclusion

In this study, we evaluated the in vitro dermal absorption of six environmentally relevant metals - arsenic, manganese, molybdenum, nickel, lead, and vanadium - from urban dust through both intact and compromised human skin. The results demonstrated that the skin acts as a dynamic and selective barrier, with metal permeation highly dependent on the physicochemical properties of each element, the pH of the surrounding medium, and the condition of the skin. In particular, Ni and Mn exhibited the highest skin permeation into the receptor fluid, suggesting a relatively high dermal bioavailability. Conversely, As and Mo displayed minimal absorption, likely due to their limited solubility and ionic mobility under the experimental conditions.

The marked increase in total metal absorption observed in damaged skin models supports the crucial role of the stratum corneum in preventing the entry of exogenous substances. Barrier disruption - whether caused by physical abrasion, dermatological disorders, or other trauma - significantly enhanced the permeability for several metals, particularly Ni, Pb, and Mn. Notably, the pronounced retention of nickel within the skin and its well-documented sensitizing potential, reinforce the importance of minimising skin contact, especially in sensitized or at-risk populations.

Comparative analysis with prior studies on road dust and stainless steel-derived particles suggests that the chemical speciation and source of particulate matter substantially affect solubility and dermal uptake. This highlights the importance of risk assessments that consider not only total metal content, but also bioavailable fractions and the actual exposure scenario.

From a preventive perspective, the results support systematic monitoring of urban dust in densely populated and high-traffic areas, particularly with regard to metals capable of inducing toxic or immunological responses. Overall, this work advances understanding of pollutant–skin interactions and contribute to the United Nations Sustainable Development Goals, particularly SDG 3 (Good Health and Well-being) and SDG 11 (Sustainable Cities and Communities), by supporting informed strategies for air pollution mitigation and human exposure prevention.

CRediT authorship contribution statement

Giovanna Marussi: Writing – original draft, Investigation, Data curation. **Francesca Larese Filon:** Writing – review & editing, Supervision, Conceptualization. **Marta Baldassar:** Investigation. **Chiara Romanello:** Investigation. **Davide Porrelli:** Investigation. **Marcella Mauro:** Conceptualization. **Nicola Zingaretti:** Resources. **Gianpiero Adami:** Supervision. **Matteo Crosera:** Writing – review & editing, Supervision, Data curation, Conceptualization.

Declaration of competing interest

The authors have no conflict of interests to disclose.

Data availability

Data will be made available on request.

References

Avasarala, Sumant, 2021. Techniques for assessing metal mobility in the environment: a geochemical perspective. In: Siegel, Malcolm, Selinus, Olle, Finkelman, Robert (Eds.), Practical Applications of Medical Geology. Springer International Publishing. https://doi.org/10.1007/978-3-030-53893-4_4.

Bronaugh, Robert L., Stewart, Raymond F., 1985. Methods for in vitro percutaneous absorption studies V: permeation through damaged skin. J. Pharm. Sci. 74 (10), 1062–1066. https://doi.org/10.1002/jps.2600741008.

Carvalho, Dayene C., Coelho, Luciana M., Acevedo, Maria Soledad M.S.F., Coelho, Nívia M.M., 2015. The oligoelements. In: Handbook of Mineral Elements in Food. John Wiley & Sons, Ltd. https://doi.org/10.1002/9781118654316.ch5.

Chaparro, Leal, Laura, T., Guney, Mert, Zagury, Gerald J., 2018. *In vitro* dermal bioaccessibility of selected metals in contaminated soil and mine tailings and human health risk characterization. Chemosphere 197 (April), 42–49. https://doi.org/10.1016/j.chemosphere.2018.01.008.

Cohen, Aaron J., Anderson, H. Ross, Ostro, Bart, Pandey, Kiran Dev, Krzyzanowski, Michal, Künzli, Nino, Gutschmidt, Kersten, Pope III, C. Arden, Romieu, Isabelle, Samet, Jonathan M., Smith, Kirk R., 2004. Urban Air Pollution. Comparative Quantification of Health Risks. World Health Organization. https://www.jstor.org/stable/resrep27829.22.

Crosera, Matteo, Adami, Gianpiero, Mauro, Marcella, Bovenzi, Massimo, Baracchini, Elena, Larese Filon, Francesca, 2016. In vitro dermal penetration of nickel nanoparticles. Chemosphere 145 (February), 301–306. https://doi.org/10.1016/j.chemosphere.2015.11.076.

Dai, Qi-Li, Bi, Xiao-Hui, Wu, Jian-Hui, Zhang, Yu-Fen, Wang, Jing, Xu, Hong, Yao, Lin, Jiao, Li, Feng, Yin-Chang, 2015. Characterization and source identification of heavy metals in ambient PM10 and PM2.5 in an integrated iron and steel industry zone

compared with a background site. Aerosol Air Qual. Res. 15 (3), 875–887. https://doi.org/10.4209/aaqr.2014.09.0226.
Dijkhoff, Irini M., Drasler, Barbara, Karakocak, Bedia Begum, Petri-Fink, Alke, Valacchi, Giuseppe, Eeman, Marc, Rothen-Rutishauser, Barbara, 2020. Impact of airborne particulate matter on skin: a systematic review from epidemiology to in vitro studies. Part. Fibre Toxicol. 17 (1), 35. https://doi.org/10.1186/s12989-020-00366-y.
Du, Xin-yue, Yu, Ya-qi, Yang, Jie, Liu, Heng-bo, Yang, Jin-yan, 2025. Cytotoxicity of vanadium(IV) and vanadium(V) on Caco-2 cells: the important influence of vanadium speciation. Biol. Trace Elem. Res. https://doi.org/10.1007/s12011-024-04506-9 (ahead of print, January 4).
Dyer, James A., Scrivner, Noel C., Dentel, Steven K., 1998. A practical guide for determining the solubility of metal hydroxides and oxides in water. Environ. Prog. 17 (1), 1–8. https://doi.org/10.1002/ep.670170112.
Erikson, Keith M., Aschner, Michael, 2003. Manganese neurotoxicity and glutamate-GABA interaction. Neurochem. Int. 43 (4), 475–480. https://doi.org/10.1016/S0197-0186(03)00037-8. Glutamine, Glutamate and GABA in the CNS: Transport and Metabolism in Health and Disease.
European Committee for Standardization (CEN), 2011. Reference Test Method for Release of Nickel from All Post Assemblies Wich Are Inserted into Pierced Parts of the Human Body and Articles Intended to Come into Direct and Prolonged Contact with the Skin. EN 1811.
Filon, Francesca Larese, Boeniger, Mark, Maina, Giovanni, Adami, Gianpiero, Spinelli, Paolo, Damian, Adriano, 2006. Skin absorption of inorganic lead (PbO) and the effect of skin cleansers. J. Occup. Environ. Med. 48 (7), 692. https://doi.org/10.1097/01.jom.0000214474.61563.1c.
Filon, Francesca Larese, D'Agostin, Flavia, Crosera, Matteo, Adami, Gianpiero, Bovenzi, Massimo, Maina, Giovanni, 2009. In vitro absorption of metal powders through intact and damaged human skin. Toxicol. in Vitro 23 (4), 574–579. https://doi.org/10.1016/j.tiv.2009.01.015.
Franken, Anja, Eloff, Frederik C., Du Plessis, Jeanetta, Du Plessis, Johannes L., 2015. In vitro permeation of metals through human skin: a review and recommendations. Chem. Res. Toxicol. 28 (12), 2237–2249. https://doi.org/10.1021/acs.chemrestox.5b00421.
Franz, T.J., Lehman, P.A., Raney, S.G., 2009. Use of excised human skin to assess the bioequivalence of topical products. Skin Pharmacol. Physiol. 22 (5), 276–286. https://doi.org/10.1159/000235828.
Guy, Richard H., 1999. Metals and the Skin: Topical Effects and Systemic Absorption. CRC Press. https://doi.org/10.1201/9780203909058.
Health Effects Institute, 2024. State of Global Air Report 2024. https://www.stateofglobalair.org/resources/report/state-global-air-report-2024.
Hostynek, Jurij J., 2003. Factors determining percutaneous metal absorption. Food Chem. Toxicol. 41 (3), 327–345. https://doi.org/10.1016/S0278-6915(02)00257-0.
Hostýnek, Jurij J., Hinz, Robert S., Lorence, Cynthia R., Price, Matthew, Guy, Richard H., 1993. Metals and the skin. Crit. Rev. Toxicol. 23 (2), 171–235.
Jin, Seon-Pil, Li, Zhenyu, Choi, Eun Kyung, Lee, Serah, Kim, Yoen Kyung, Seo, Eun Young, Chung, Jin Ho, Cho, Soyun, 2018. Urban particulate matter in air pollution penetrates into the barrier-disrupted skin and produces ROS-dependent cutaneous inflammatory response *in vivo*. J. Dermatol. Sci. 91 (2), 175–183. https://doi.org/10.1016/j.jdermsci.2018.04.015.
Julander, Anneli, Midander, Klara, Garcia-Garcia, Sandra, Vihlborg, Per, Graff, Pål, 2020. A case study of brass foundry workers' estimated lead (Pb) body burden from different exposure routes. Ann. Work Expo. Health 64 (9), 970–981. https://doi.org/10.1093/annweh/wxaa061.
Kaonga, Chikumbusko Chiziwa, Kosamu, Ishmael Bobby Mphangwe, Utembe, Wells Robert, 2021. A review of metal levels in urban dust, their methods of determination, and risk assessment. Atmosphere 12 (7), 7. https://doi.org/10.3390/atmos12070891.
Katsnelson, Boris A., Minigaliyeva, Ilzira A., Panov, Vladimir G., Privalova, Larisa I., Varaksin, Anatoly N., Gurvich, Vladimir B., Sutunkova, Marina P., Shur, Vladimir Ya., Shishkina, Ekaterina V., Valamina, Irene E., Makeyev, Oleg H., 2015. 'Some patterns of metallic nanoparticles' combined subchronic toxicity as exemplified by a combination of nickel and manganese oxide nanoparticles'. Food Chem. Toxicol. 86 (December), 351–364. https://doi.org/10.1016/j.fct.2015.11.012.
Kelly, Frank J., Fussell, Julia C., 2012. Size, source and chemical composition as determinants of toxicity attributable to ambient particulate matter. Atmos. Environ. 60 (December), 504–526. https://doi.org/10.1016/j.atmosenv.2012.06.039.
Kezic, Sanja, Nielsen, J.B., 2009. Absorption of chemicals through compromised skin. Int. Arch. Occup. Environ. Health 82 (6), 677–688. https://doi.org/10.1007/s00420-009-0405-x.
Kim, Byung Eui, Kim, Jihyun, Goleva, Elena, Berdyshev, Evgeny, Lee, Jinyoung, Vang, Kathryn A., Lee, Un Ha, Han, SongYi, Leung, Susan, Hall, Clifton F., Kim, Na-Rae, Bronova, Irina, Lee, Eu Jin, Yang, Hye-Ran, Leung, Donald Y.M., Ahn, Kangmo, 2021. Particulate matter causes skin barrier dysfunction. JCI Insight 6 (5), e145185. https://doi.org/10.1172/jci.insight.145185.
Lansdown, Alan B.G., 1995. Physiological and toxicological changes in the skin resulting from the action and interaction of metal ions. Crit. Rev. Toxicol. 25 (5), 397–462. https://doi.org/10.3109/10408449509049339.
Larese Filon, Francesca, 2018. Penetration of metals through the skin barrier. In: Chen, Jennifer K., Thyssen, Jacob P. (Eds.), Metal Allergy: From Dermatitis to Implant and Device Failure. Springer International Publishing. https://doi.org/10.1007/978-3-319-58503-1_7.
Larese Filon, Francesca, Bello, Dhimiter, Cherrie, John W., Sleeuwenhoek, Anne, Spaan, Suzanne, Brouwer, Derk H., 2016. Occupational dermal exposure to nanoparticles and nano-enabled products: part I—factors affecting skin absorption. Int. J. Hyg. Environ. Health 219 (6), 536–544. https://doi.org/10.1016/j.ijheh.2016.05.009.
Larese Filon, Francesca, Marussi, Giovanna, Payet, Mickael, Debellemaniere, Olivier, Parodi, Pier Camillo, Zingaretti, Nicola, Malard, Veronique, Lebaron-Jacobs, Laurence, Adami, Gianpiero, Mauro, Marcella, Pavoni, Elena, Crosera, Matteo, 2025. Skin absorption of metals derived from hydrogenated stainless particles in human skin: results from the TITANS project. Environ. Pollut. 364 (January), 125327. https://doi.org/10.1016/j.envpol.2024.125327.
Larese, Francesca, Gianpietro, Adami, Venier, Marta, Maina, Giovanni, Renzi, Nadia, 2007. In vitro percutaneous absorption of metal compounds. Toxicol. Lett. 170 (1), 49–56. https://doi.org/10.1016/j.toxlet.2007.02.009.
Lilley, S.G., Florence, T.M., Stauber, J.L., 1988. The use of sweat to monitor lead absorption through the skin. Sci. Total Environ. 76 (2), 267–278. https://doi.org/10.1016/0048-9697(88)90112-X.
Magnano, Greta Camilla, Marussi, Giovanna, Pavoni, Elena, Adami, Gianpiero, Filon, Francesca Larese, Crosera, Matteo, 2022. Percutaneous metals absorption following exposure to road dust powder. Environ. Pollut. 292 (January), 118353. https://doi.org/10.1016/j.envpol.2021.118353.
Magnano, Greta Camilla, Marussi, Giovanna, Crosera, Matteo, Hasa, Dritan, Adami, Gianpiero, Lionetti, Nicola, Filon, Francesca Larese, 2024. Probing the effectiveness of barrier creams against human skin penetration of nickel powder. Int. J. Cosmet. Sci. 46 (1), 39–50. https://doi.org/10.1111/ics.12893.
Malmberg, Per, Guttenberg, Thomas, Ericson, Marica B., Hagvall, Lina, 2018. Imaging mass spectrometry for novel insights into contact allergy – a proof-of-concept study on nickel. Contact Dermatitis 78 (2), 109–116. https://doi.org/10.1111/cod.12911.
Marin Villegas, Carlos A., Zagury, Gerald J., 2021. Comparison of synthetic sweat and influence of sebum in the permeation of bioaccessible metal(loid)s from contaminated soils through a synthetic skin membrane. Environ. Sci. Technol. 55 (12), 8215–8222. https://doi.org/10.1021/acs.est.1c02038.
Marin Villegas, Carlos A., Zagury, Gerald J., 2023a. Incorporating oral, inhalation and dermal bioaccessibility into human health risk characterization following exposure to chromated copper arsenate (CCA)-contaminated soils. Ecotoxicol. Environ. Saf. 249 (January), 114446. https://doi.org/10.1016/j.ecoenv.2022.114446.
Marin Villegas, Carlos A., Zagury, Gerald J., 2023b. Metal(loid) speciation in dermal bioaccessibility extracts from contaminated soils and permeation through synthetic skin. J. Hazard. Mater. 455 (August), 131523. https://doi.org/10.1016/j.jhazmat.2023.131523.
Marin Villegas, Carlos A., Guney, Mert, Zagury, Gerald J., 2019. Comparison of five artificial skin surface film liquids for assessing dermal bioaccessibility of metals in certified reference soils. Sci. Total Environ. 692 (November), 595–601. https://doi.org/10.1016/j.scitotenv.2019.07.281.
OECD, 2004. Test no. 428: skin absorption. In: Vitro Method. Section 4. OECD Publishing. https://doi.org/10.1787/9789264071087-en.
OECD, 2018. Guidance Document on Good In Vitro Method Practices (GIVIMP). OECD Series on Testing and Assessment. OECD. https://doi.org/10.1787/9789264304796-en.
Ouypornkochagorn, Sairoong, Feldmann, Jörg, 2010. Dermal uptake of arsenic through human skin depends strongly on its speciation. Environ. Sci. Technol. 44 (10), 3972–3978. https://doi.org/10.1021/es903667y.
Owen, Joshua L., Vakharia, Paras P., Silverberg, Jonathan I., 2018. The role and diagnosis of allergic contact dermatitis in patients with atopic dermatitis. Am. J. Clin. Dermatol. 19 (3), 293–302. https://doi.org/10.1007/s40257-017-0340-7.
Pan, Tai-Long, Wang, Pei-Wen, Al-Suwayeh, Saleh A., Chen, Chih-Chieh, Fang, Jia-You, 2010. Skin toxicology of lead species evaluated by their permeability and proteomic profiles: a comparison of organic and inorganic lead. Toxicol. Lett. 197 (1), 19–28. https://doi.org/10.1016/j.toxlet.2010.04.019.
Rehder, Dieter, 2013. Vanadium. Its role for humans. In: Sigel, Astrid, Sigel, Helmut, Sigel, Roland K.O. (Eds.), Interrelations Between Essential Metal Ions and Human Diseases. Springer Netherlands. https://doi.org/10.1007/978-94-007-7500-8_5.
Rizzo, Marco, Bordignon, Michele, Bertoli, Paolo, Biasiol, Giorgio, Crosera, Matteo, Magnano, Greta Camilla, Marussi, Giovanna, Negro, Corrado, Filon, Francesca Larese, 2024. Exposure to gallium arsenide nanoparticles in a research facility: a case study using molecular beam epitaxy. Nanotoxicology 18 (3), 259–271. https://doi.org/10.1080/17435390.2024.2341893.
Rizzo, Marco, Marussi, Giovanna, Crosera, Matteo, Marcella, Mauro, Biasiol, Giorgio, Adami, Gianpiero, Magnano, Greta Camilla, Filon, Francesca Larese, 2025. Gallium and arsenic human skin permeation after application of GaAs particles: an *ex-vivo* study using Franz cells. Food Chem. Toxicol. 206 (December), 115758. https://doi.org/10.1016/j.fct.2025.115758.
Roy, Sayantee, Gupta, Sanjay Kumar, Prakash, Jai, Habib, Gazala, Kumar, Prashant, 2022. A global perspective of the current state of heavy metal contamination in road dust. Environ. Sci. Pollut. Res. 29 (22), 33230–33251. https://doi.org/10.1007/s11356-022-18583-7.
Simon, Konstantin, Reichardt, Philipp, Luch, Andreas, Roloff, Alexander, Siewert, Katherina, Riedel, Franziska, 2024. Less efficient skin penetration of the metal allergen Pd2+ compared to Ni2+ and Co2+ from patch test preparations. Contact Dermatitis 91 (1), 11–21. https://doi.org/10.1111/cod.14569.
Song, Sanghwan, Lee, Kiyoung, Lee, Young-Mi, Lee, Young-Mi, Lee, Jung-Hyun, Lee, Sang Il, Yu, Seung-Do, Paek, Domyung, 2011. Acute health effects of urban fine and ultrafine particles on children with atopic dermatitis. Environ. Res. 111 (3), 394–399. https://doi.org/10.1016/j.envres.2010.10.010.
Stauber, J.L., Florence, T.M., Gulson, B.L., Dale, L.S., 1994. Percutaneous absorption of inorganic lead compounds. Sci. Total Environ. 145 (1), 55–70. https://doi.org/10.1016/0048-9697(94)90297-6.

Sun, Chee-Ching, Wong, Ten-Tsao, Hwang, Yaw-Huei, Chao, Kun-Yu, Jee, Shiou-Hwa, Wang, Jung-Der, 2002. Percutaneous absorption of inorganic lead compounds. AIHA J. 63 (5), 641–646. https://doi.org/10.1080/15428110208984751.

Thyssen, Jacob P., Menné, Torkil, 2010. Metal allergy—a review on exposures, penetration, genetics, prevalence, and clinical implications. Chem. Res. Toxicol. 23 (2), 309–318. https://doi.org/10.1021/tx9002726.

US EPA, 1996. EPA Method 3052: Microwave Assisted Acid Digestion of Siliceous and Organic Matrices. United States Environmental Protection Agency. https://www.epa.gov/sites/default/files/2015-12/documents/3052.pdf.

Vierkötter, Andrea, Schikowski, Tamara, Ranft, Ulrich, Sugiri, Dorothea, Matsui, Mary, Krämer, Ursula, Krutmann, Jean, 2010. Airborne particle exposure and extrinsic skin aging. J. Invest. Dermatol. 130 (12), 2719–2726. https://doi.org/10.1038/jid.2010.204.

World Health Organization, 2006. Dermal Absorption. Published under the Joint Sponsorship of the United Nations Environment Programme, the International Labour Organisation and the World Health Organization, and Produced within the Framework of the Inter-Organization Programme for the Sound Management of Chemicals, 235. Environmental health criteria, Geneva. https://iris.who.int/handle/10665/43542.